ELSEVIER

Contents lists available at ScienceDirect

Biomaterials

journal homepage: www.elsevier.com/locate/biomaterials



The nano-morphological relationships between apatite crystals and collagen fibrils in ivory dentine

V. Jantou-Morris^a, Michael A. Horton^b, David W. McComb^{a,*}

ARTICLE INFO

Article history: Received 24 February 2010 Accepted 9 March 2010 Available online 9 April 2010

Keywords: Ivory dentine Collagen D banding Apatite FIB milling HAADF-STEM FFI S

ABSTRACT

In this work, analytical transmission electron microscopy (TEM) was used to study the nanostructure of mineralised ivory dentine, in order to gain a clearer understanding of the relationship between the organic (collagen fibrils) and inorganic (calcium phosphate apatite crystals) components. Thin sections prepared by both focused ion beam (FIB) milling and ultramicrotomy, in the longitudinal and transverse planes, were investigated using electron energy-loss spectroscopy (EELS) in a monochromated field-emission gun scanning TEM (FEI Titan 80-300 FEGSTEM). Both low- and core-loss spectroscopy were used in the investigation, and the signals from phosphorous, carbon, calcium, nitrogen and oxygen were studied in detail. A combination of HAADF (high-angle annular dark-field)-STEM imaging and EELS analysis was used for simultaneous acquisition of both spatial and spectral information pixel by pixel (spectrum imaging). Across the collagen *D* banding in longitudinal sections, the relative thickness of the bright bands was significantly higher than that of the dark bands. Core-loss spectroscopy showed that the bright bands were richer in apatite than the dark bands. However, no ELNES variation was observed across the *D* banding. In transverse sections, significant changes in the carbon edge fine structure were observed at the interface between the extra- and intra-fibrillar regions.

© 2010 Elsevier Ltd. All rights reserved.

1. Introduction

The need to characterise the structure and chemistry of mineralised tissues at the nanometre and sub-nanometre scale stems in part from the increasing number of bone related pathologies in our ageing society. In order to gain a better understanding of the mechanical properties of mineralised tissues and how these are affected by skeletal disorders, it is necessary to examine the relationship between the two major constituents: calcium phosphate apatite crystals (Ca₅(PO₄)₃OH) and type-I collagen fibrils [1,2]. Although the macro- and micro-structures of mineralised tissues have become well known, the inherent complexity of such specimens makes investigation and understanding of the nanostructure challenging. One particular controversial subject is the origin of a periodic contrast, characteristic of TEM (and AFM) images of collagen fibrils. This is often referred to as the collagen "D banding", D being the 64-67 nm periodicity of this feature [2-5]. Each D period is divided into two regions: bright and dark bands, the denomination of "bright" and "dark" being based on a high and low intensity respectively in bright-field TEM (BFTEM) images. The

banding is thought to arise from the arrangement of the collagen molecules forming the fibrils: based on the widely accepted Hodge and Petruska model [6], collagen molecules assemble in a quarter-staggered array, leading to the creation of gap (40 nm) and overlap (27 nm) regions. The gaps are thought to accommodate the apatite crystals and therefore appear dark on the TEM image, whilst the overlap regions are made of collagen only and appear as the bright bands. TEM images of ivory dentine sections prepared in the transverse plane revealed distinct circular features with dark "needles" surrounding a brighter interior region [7]. These features are believed to be the collagen fibrils viewed in cross-section.

The work presented here is concerned with the structural and chemical analyses of ivory dentine, using electron energy-loss spectroscopy (EELS) in the (scanning) transmission electron microscope ((S)TEM). STEM-EELS is a unique tool for structural and chemical characterisation of materials at the nanometre scale [8]. Samples were prepared in the longitudinal and transverse planes using two different techniques, ultramicrotomy and focused ion beam (FIB) milling, which have been described elsewhere [7]. Both the low- and core-loss regions of the EEL spectrum were used to characterise the samples. Low-loss spectroscopy was carried out to investigate changes in the plasmon peak shape and to plot the relative thickness. Core-loss spectroscopy was used to investigate compositional differences and to look for variations in the

^a London Centre for Nanotechnology and Department of Materials, Imperial College London, London SW7 2AZ, UK

^b London Centre for Nanotechnology and Department of Medicine, University College London, London WC1H 0AH, UK

^{*} Corresponding author.

E-mail address: d.mccomb@imperial.ac.uk (D.W. McComb).

energy-loss near-edge structure (ELNES) of the five elements of interest. The specific excitations considered are the K-edges of carbon (284 eV), nitrogen (400 eV) and oxygen (532 eV) and the $L_{2,3}$ -edges of phosphorus (132 eV) and calcium (346–350 eV) [9].

2. Materials and methods

2.1. Mineralised ivory dentine

Ivory dentine from elephant tusk of an adult male was chosen for this work (the samples were confiscated at point of entry to the UK; kindly provided by HM Customs and Excise, London Heathrow Airport). Ivory dentine contains the same two basic constituents as bone (i.e. type-I collagen fibrils and apatite crystals) in similar proportions and therefore acts as a good model for bone [10–13]. The microstructure of ivory is simpler than that of bone, the long axis of the collagen fibrils being oriented in the same direction as the long axis of the tusk [12]. The investigation of the apatite/collagen relationship is therefore facilitated as sections can easily be produced either along or across the long axis of the collagen fibrils, i.e. in the longitudinal and transverse planes respectively. In longitudinal sections, the long axis of collagen fibrils is parallel to the plane of the sections, whereas in transverse sections, it is perpendicular to the plane of the section.

2.2. Sample preparation

Samples were prepared using ultramicrotomy and focused ion beam (FIB) milling following the procedures described previously [7]. In order to minimise hydrocarbon contamination during HAADF-STEM imaging and EELS analysis, samples were plasma cleaned prior analysis for 10–12 s in a plasma cleaner (Gatan Solarus 950) using a gas mixture of (H₂,O₂).

2.3. Analytical electron microscopy

Sections were investigated using EELS in a monochromated FEG-(S)TEM (FEI Titan 80-300), equipped with a double-hexapole aberration corrector for the objective lens. The Titan is also equipped with an electron energy-loss spectrometer (Gatan Tridiem 865). EELS analysis was carried out in HAADF (high-angle annular dark-field)-STEM mode, using both point spectroscopy and spectrum imaging, where data were acquired by automatically stepping the electron probe from one pixel to the next. Drift correction algorithms were used to ensure spatial correlation between spectral and image information. Care was taken to analyse areas of the samples which were not situated above the holey carbon support film of the TEM, to prevent it from contributing to the shape of the edges.

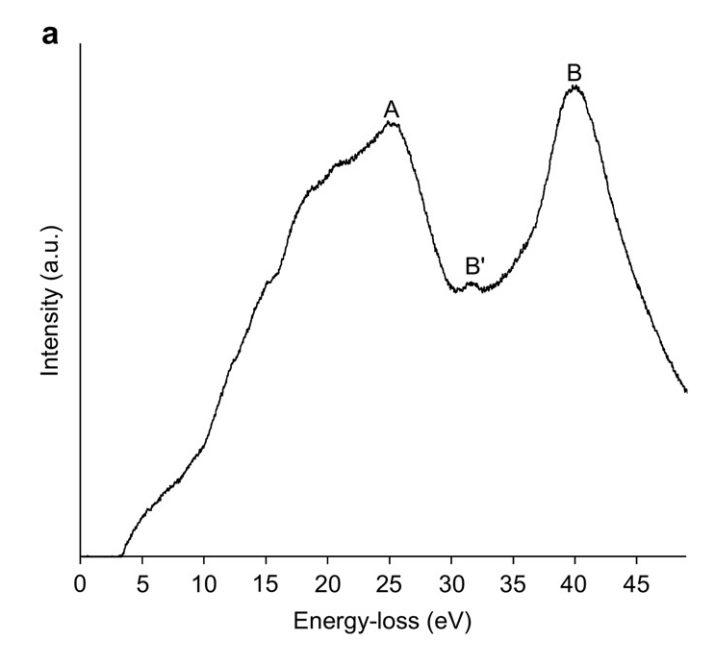
The Titan was operated at 300 kV with an extraction voltage of 3800 V. In HAADF-STEM mode, the condenser apertures were set to C1 = 2000 μm and C2 = 50 μm with a spot size of 6. This setting resulted in a probe size of approximately 0.6 nm and a convergence semi-angle (α) of 10 mrad. The HAADF detector inner collection angle was approximately 77 mrad, ensuring that diffraction contribution to the image was negligible. The contrast between the lighter and darker regions of HAADF-STEM images therefore arises either from a change in the atomic number (Z) or thickness (t). During EELS analysis, the dispersion of the spectrometer and the acquisition time were 0.1 eV/pixel and 0.06 s respectively for low-loss spectroscopy, and 0.3 eV/pixel and 10 s for core-loss spectroscopy ensuring that all five edges of interest fit in one single spectrum. A collection semi-angle (β) of \approx 11 mrad was used for core-loss spectroscopy. The energy resolution was typically 0.2 eV and 0.65–0.75 eV for monochromated and non-monochromated beams, respectively.

3. Results

3.1. Overall shape of the low-loss spectrum

A typical low-loss spectrum from ivory dentine (Fig. 1a) exhibits two broad peaks, labelled A and B, at 25.8 eV and 39.6 eV respectively, with a weak pre-peak feature, B', at 31 eV. Peaks B and B' correspond to the calcium $M_{2,3}$ -edge [9]. This overall shape was consistently observed; the main differences observed between spectra from different regions of the sample were the appearance of fine structure on the low-energy side of peak A and variations in the intensity of peak B.

The spectra were deconvolved to remove contributions from plural scattering using the Fourier-log method. The single scattering distributions (SSDs) obtained are proportional to $\text{Im}[-1/\varepsilon(E)]$, where $\varepsilon(E) = \varepsilon_1(E) + i\varepsilon_2(E)$ is the complex dielectric function [8,14]. ε_1 provides information on the collective electron excitations,



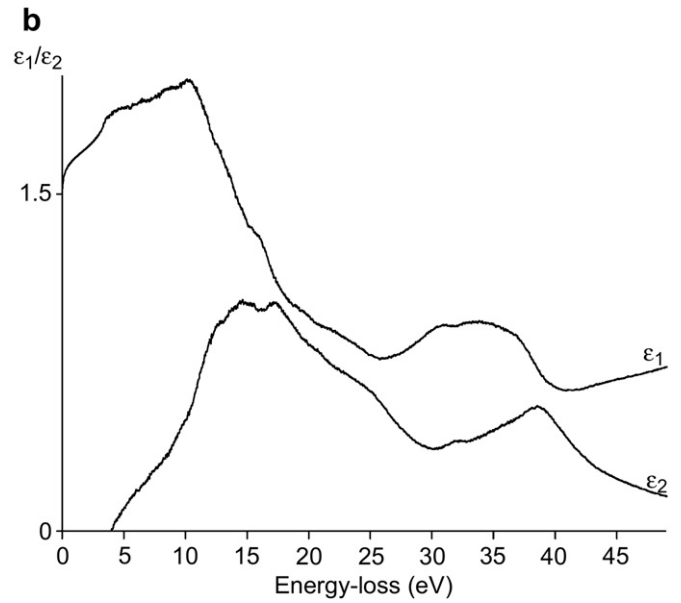


Fig. 1. a) Typical monochromated low-loss spectrum of ivory dentine after deconvolution; peak A corresponds to the plasmon peak whereas peaks B and B' correspond to the calcium $M_{2,3}$ -edge. b) Real (ε_1) and imaginary (ε_2) part of the complex dielectric function obtained from Kramers–Kronig analysis of the EEL spectrum.

whereas ε_2 relates to single electron transitions. Kramers–Kronig (KK) analysis, normalised using a refractive index of 1.5, was used to calculate ε_1 and ε_2 from the SSDs to establish if the features in the low-energy region were single electron-like. Plots of ε_1 and ε_2 confirm that the bulk plasmon in ivory dentine apatite crystals lies at 25.8 eV, corresponding to peak A (Fig. 1b). Fine structure on the ε_2 plot, indicative of single electron transitions, can be seen at the following energies: 12 eV, 12.8 eV, 13.7 eV, 14.8 eV and 16.4 eV.

Comparison of the low-loss data across the banding (Fig. 2) revealed subtle differences at low energy-losses: whilst no fine structure was seen on the low-loss spectrum of the (HAADF-STEM) dark bands, a peak situated at approximately 17.2 eV appeared on the plasmon peak shoulder of the (HAADF-STEM) bright bands. KK analysis suggests that this feature arises from single electron transitions.

Download English Version:

https://daneshyari.com/en/article/8391

Download Persian Version:

https://daneshyari.com/article/8391

<u>Daneshyari.com</u>